Hindawi
Advances in Polymer Technology
Volume 2020, Article ID 3481752, 11 pages
https://doi.org/10.1155/2020/3481752

Research Article

Study of Residual Wall Thickness and Multiobjective Optimization for Process Parameters of Water-Assisted Injection Molding

Jiangen Yang[1], **Shengrui Yu**[2] **and Ming Yu**[3]

[1]*Engineering Science and Technology Department, Shanghai Ocean University, Shanghai 201306, China*
[2]*Mechanical and Electronic Engineering Department, Jingdezhen Ceramic Institute, Jingdezhen 333403, China*
[3]*School of Materials Science and Engineering, Jiangsu University of Science and Technology, Zhenjiang 212000, China*

Correspondence should be addressed to Jiangen Yang; jgyang@shou.edu.cn

Received 31 May 2020; Revised 27 October 2020; Accepted 5 December 2020; Published 11 December 2020

Academic Editor: Rafael Mu oz Esp

Residual wall thickness is an important indicator for water-assisted injection molding (WAIM) parts, especially the maximization of hollowed core ratio and minimization of wall thickness difference which are significant optimization objectives. Residual wall thickness was calculated by the computational fluid dynamics (CFD) method. The response surface methodology (RSM) model, radial basis function (RBF) neural network, and Kriging model were employed to map the relationship between process parameters and hollowed core ratio, and wall thickness difference. Based on the comparison assessments of the three surrogate models, multiobjective optimization of hollowed core ratio and wall thickness difference for cooling water pipe by integrating design of experiment (DOE) of optimized Latin hypercubes (Opt LHS), RBF neural network, and particle swarm optimization (PSO) algorithm was studied. The research results showed that short shot size, water pressure, and melt temperature were the most important process parameters affecting hollowed core ratio, while the effects of delay time and mold temperature were little. By the confirmation experiments for the best solution resulted from the Pareto frontier, the relative errors of hollowed core ratio and wall thickness are 2.2% and 3.0%, respectively. It demonstrated that the proposed hybrid optimization methodology could increase hollowed core ratio and decrease wall thickness difference during the WAIM process.

1. Introduction

WAIM, one of the innovations of plastic injection molding technology, is the newest way to mold hollow parts. The development of this molding technique is a variant of gas-assisted injection molding, which has the main strength of reducing part costs and improving part characteristics. However, because of water instead of gas as a molding medium, there are some unique advantages in WAIM: thin residual wall thickness, smooth inner surface, and short cycle. By far, some automotive plastic products, such as foot pedals, handrails, and engine cooling water pipes, are made by WAIM.

Residual wall thickness is one of the most important indexes of part quality, which significantly affects the strength. Some scholars have conducted studies on how to improve the residual wall thickness from the aspects of water needle structure, process parameters, auxiliary media, and cavity cross-sectional shape. Park et al. [1] used numerical simulation and experimental methods to study the effect of process parameters on the residual wall thickness of product and found that an important reason for the uneven residual wall thickness was the unstable flow caused by the boiling of water in the mold cavity. Kuang et al. [2] studied the influence of cavity cross-sectional shape on water penetration, and the results showed that residual wall thickness distribution of circular pipe was relatively uniform, while for noncircular pipe, there was the largest residual wall thickness at the position far away from the center of the section. Park et al. [3, 4] separately used water and silicone oil for assisted injection molding, analyzed the generation mechanism of wall thickness difference, and effectively controlled

the void of product and concentricity of wall thickness distribution. Sannen et al. [5] studied wall thickness defects of product and improved quality through the adjustment of process parameters. Kuang et al. [6] used an improved warhead device to study the effect of process parameters on residual wall thickness. These studies were based on the effect between different molding parameters and residual wall thickness, which have laid a solid foundation for the improvement of residual wall thickness.

However, the relationship between molding parameters and residual wall thickness is highly complex. In particular, the optimization of process parameters can be more feasible and reasonable to meet the requirement of product quality with the advantages of saving on materials and energy [7]. In recent years, there are widespread attentions for plastic injection molding optimization based on optimal design theory; more details on optimization theory and application can be found in an early study [8]. While compared with the many optimization techniques used in traditional injection molding, the optimization studies related to WAIM are few. Liu and Chen [9] and Huang and Deng [10] used the orthogonal experiment method to study the effect of process parameters on water penetration length and optimized process parameters to determine the largest water penetration length. Yang et al. [11] put forward a combined optimization strategy that integrated orthogonal experimental design, surrogate model, and optimization algorithm. Through the optimization of process parameters, the maximum water penetration length was obtained, which was obviously superior than orthogonal optimization. Zhou et al. [12] mapped the relationship between process parameters and standard deviation depicting residual wall thickness uniformity with surrogate model optimized by a genetic algorithm and found the best performance for predicting standard deviation. However, the evaluation of product quality is multifaceted, and single-objective optimization is difficult to meet the actual product quality requirements. Most of the researches are based on hypothetical polymer products. Therefore, in this paper, the research object is an engine cooling water pipe made of polymer material, which will provide a reference for the similar work, especially for the selection of polymer materials. In addition, the two indicators of hollowed core ratio and wall thickness difference, comprehensively evaluating residual wall thickness, are used as multiobjective optimization applications. To the best knowledge of authors, multiobjective optimization for WAIM has not ever been studied.

In this paper, the main research was devoted to present an integrated optimization strategy, DOE of Opt LHS, surrogate model, and PSO algorithm, to find the optimal process parameters resulting in maximizing hollowed core ratio and minimizing wall thickness difference. This paper studied the following: (1) the DOE of Opt LHS, and calculating of residual wall thickness by CFD; (2) the building of RSM, RBF, and Kriging models, and cross-validation; (3) the effects of process parameters on hollowed core ratio; and (4) the multiobjective optimization for maximizing hollowed core ratio and minimizing wall thickness difference, and verification. Now, we are working together with Xunyu Mould Co. Ltd of Ningbo to develop WAIM technology. For engine cooling water pipe, we have set up experimental equipment of WAIM including an injection-molding machine, a mold, and water auxiliary injection devices. The integrated optimization strategy that aims for better molding quality of plastic product is helpful to accelerate the development of optimization technology in WAIM and will lay a good foundation for future industrial applications.

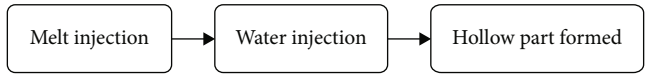

Figure 1: WAIM process.

2. Model and Method

The basic process of WAIM is shown in Figure 1, which goes as follows: firstly, the high-temperature melt is injected into the mold cavity; then, water is injected after a certain delay time, which pushes high-temperature melt forward; finally, the hollow part is formed.

2.1. Mathematical Model. In WAIM, the filling process is non-Newtonian laminar of polymer melt and turbulence of water with high Reynolds number. What makes WAIM different from traditional injection molding is that the injection of water is turbulence, and the interchange of heat between water and melt is obvious. Based on the generalized Hele-Shaw model, the improved Reynolds time-averaged motion equation including Reynolds stresses is

$$\frac{\partial(\rho u_i)}{\partial t} + \frac{\partial(\rho u_i u_j)}{\partial x_j} = -\frac{\partial p}{\partial x_i} + \frac{\partial}{\partial x_j}\left(\mu \frac{\partial u_i}{\partial x_j}\right) - \frac{\partial}{\partial x_j}\left(\rho \overline{u_i}' u_j'\right), \tag{1}$$

where the last item is Reynolds stresses.

According to Boussinesq eddy viscosity assumption, Reynolds stresses is solved by the following equation:

$$-\rho \overline{u_i}' u_j' = \mu_t \left(\frac{\partial u_i}{\partial x_j} + \frac{\partial u_j}{\partial x_i}\right) - \frac{2}{3}\left(\rho\kappa + \mu \frac{\partial u_i}{\partial x_j}\right)\delta_{ij}, \tag{2}$$

where μ_t is the turbulent viscosity; κ is the turbulent kinetic energy.

Simulated by the standard $k-\varepsilon$ model, the solving method for μ_t is

$$\mu_t = \rho C_\mu \frac{\kappa^2}{\varepsilon}, \tag{3}$$

where C_μ is the empirical constant and ε is the dissipation rate.

More details on the mathematical model of WAIM can be found in the author's early study [13].

2.2. Surrogate Model. The surrogate model is based on experimental design and statistical analysis and is an alternative model method for reflecting real problems. There are some

advantages for the surrogate model, such as small calculation amount, and high accuracy, which can ensure that the optimization algorithm searches for the optimal solution in the continuous space of design variables. At present, in the field of plastic injection molding, RSM, RBF, and Kriging models are frequently used [8].

2.2.1. RSM Model. The basic idea of the RSM model is to fit a response surface through a series of deterministic experiments, thereby expressing the complex relationship between multifactor input and output in a system. The model is essentially a polynomial function, which can be fitted by four orders. In general, the higher the polynomial order is, the more accurate the fitted response surface model will be. Moreover, it combines experiment design and mathematical modeling with the advantages of less test times and good predictive performance and can fit some complex response relationship in plastic injection molding [14, 15].

The usual first-order and second-order polynomial equations are expressed by

$$\begin{aligned} \tilde{y}(x) &= \beta_0 + \sum_{i=1}^{M} \beta_i x_i, \\ \tilde{y}(x) &= \beta_0 + \sum_{i=1}^{M} \beta_i x_i + \sum_{i=1}^{M} \beta_{ii} x_i^2 + \sum_{i \neq j}^{M} \beta_{ij} x_i x_j, \end{aligned} \tag{4}$$

where β_0 denotes the intercept constant; β_i, β_{ii}, and β_{ij} denote the coefficients of the first, second, and cross terms, respectively; x_i and x_j denote design variables; M denotes the numbers of design variables.

The term selection method can be used to choose some important polynomial terms and discard some less important polynomial terms for improving the reliability of the model. It includes sequential replacement, stepwise, two-at-a-time replacement, and exhaustive search, which take the smallest residual sum of squares (RSS) as the goal to select the best item. The formula for RSS is as follows:

$$\mathrm{RSS} = \sum_{i=1}^{n} (y_i - y\wedge_i)^2, \tag{5}$$

where n is the number of sample points that construct the RSM model; i is the ith sample; y_i is the actual value of the sample; $\widehat{y}_i$ is the predicted value of the RSM model.

2.2.2. RBF Model. RBF neural network is an effective fitting model, which is widely used in fitting highly complex nonlinear problems. Li et al. [16] introduced a modified global optimization method based on the RBF surrogate model and its application in packing profile optimization of injection molding process; Kitayama et al. [17] presented sequential approximate optimization using the RBF network for minimizing weldlines and clamping force; Heidari et al. [18] used RBF coupled with a cross-validation technique to minimize volumetric shrinkage and warpage. The RBF neural network includes a three-layer forward network, namely, input layer, hidden layer, and output layer. The relationship between the three layers is as follows: the input layer is converted to the hidden layer through a fixed nonlinear transformation; the hidden layer space is mapped to the output layer through linear transformation.

The basis function of the RBF model is a radial function, and the construction method is linear superposition. Assuming input X and output Y, RBF is expressed as follows:

$$f(x) = \sum_{i=1}^{n} \omega_i \phi(r^i) = \sum_{i=1}^{n} \omega_i \phi(\|x - x^i\|), \tag{6}$$

where ω_i is the weight coefficient; r^i is the Euclidean distance; $\phi(r^i)$ is the nonlinear radial basis function.

According to the interpolation $f(x^j) = y^j$, the following equations can be obtained:

$$\Phi(\|x^i - x^j\|) \cdot \omega = Y. \tag{7}$$

When $\phi(r^i)$ is a positive definite function and the sample points do not coincide, the above formula has a unique solution:

$$\omega = \Phi(\|x^i - x^j\|)^{-1} \cdot Y. \tag{8}$$

There are many basis functions, of which the Gaussian function is the most common one, namely,

$$\phi(r) = \mathrm{e}^{-r^2/c^2}, \tag{9}$$

where c is a constant greater than 0.

2.2.3. Kriging Model. Geologist Krige first proposes the Kriging model, which is based on structural analysis and variation function theory and can unbiasedly optimize the design of regionalized variables [19]. In the early period, the Kriging method was mainly used to estimate the reserve distribution of mineral deposits, and gradually, it was applied to the multiscientific optimized design. The input variables and response values of the Kriging model can be determined by the following formula:

$$y(x) = f(x) + \mu(x), \tag{10}$$

where $f(x)$ is a fixed item of the known polynomial function x; $\mu(x)$ is an approximate random function reflecting the local difference; the mean is 0; σ_μ^2 is variance, and the covariance matrix is

$$Cov[\mu(v), \mu(w)] = \sigma_\mu^2 [R(\theta, V, W)], \tag{11}$$

where $R(\theta, V, W)$ is the correlation function of the sampling points V and W with the parameter θ.

Under the condition of small samples, a certain fitting accuracy can be ensured by the Kriging model, which has been well applied to the part stiffness predictions [20], and the reducing of part residual stress and warpage [21].

Through the effect of the correlation function, the characteristic of optimization design is a local estimation.

2.3. PSO Algorithm. PSO is an evolutionary optimization algorithm developed by Kennedy and Eberhart, which has been successfully applied in the optimization design of plastic injection molding, including the optimization studies of volumetric shrinkage of biaspheric lens [22], product design time forecast [23], and product weight control [24].

The PSO algorithm is based on a group of particles. Assuming that a group of m particles flies in the D-dimensional space, the position of the ith particle is expressed as follows:

$$X_i = (x_{i1}, x_{i2}, \cdots, x_{iD}). \tag{12}$$

The velocity of the ith particle is represented as

$$V_i = (v_{i1}, v_{i2}, \cdots, v_{iD}). \tag{13}$$

During each iteration of the particle swarm, each particle must not only find its own historical best point (pbest) but also search for the best historical point of other particles (gbest). The individual extreme of pbest is expressed as

$$P_i = (p_{i1}, p_{i2}, \cdots, p_{iD}). \tag{14}$$

The global extreme of gbest is expressed as

$$P_g = \left(p_{g1}, p_{g2}, \cdots, p_{gD}\right). \tag{15}$$

After determining X_i, V_i, pbest, and gbest, the particle's D-dimensional position (x_{id}) and velocity (v_{id}) are updated according to the following formula:

$$\begin{aligned} x_{id} &= x_{id} + v_{id}, \\ v_{id} &= \omega v_{id} + c_1 r_1 (p_{id} - x_{id}) + c_2 r_2 \left(p_{gd} - x_{id}\right), \end{aligned} \tag{16}$$

where the first term gives particles a tendency to expand the search space, which is an inertial term; the second term represents the particle's own direction of improvement, which is a cognitive term; the third term represents the information that is optimally shared between particles and is a social term; ω is the inertial weight; c_1 and c_2 are positive acceleration constants; r_1 and r_2 are random numbers distributed between 0 and 1.

2.4. Optimization Flow. By the hybrid DOE, surrogate model, and optimization technique, the optimization design process of this problem is shown in Figure 2. The main steps are as follows:

2.4.1. Determine the Experimental Design Method. The experimental product is a brand of automobile cooling water pipe, of which the cross-section is round and precise, the outer diameter is 29 mm, the average wall thickness is 2 mm, and the length is about 400 mm, as shown in Figure 3. The original product is a metal pipe fitting, which is processed by multiple processes such as bending, necking, extrusion, and bracket welding. The process steps are numerous and complicated, which results in low efficiency and high cost.

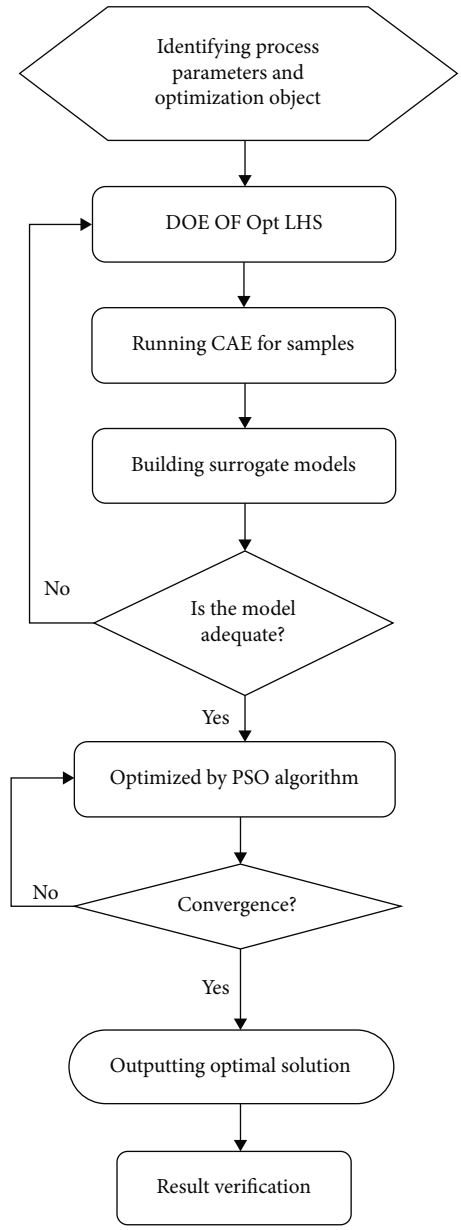

Figure 2: Flow chart of hybrid optimization design.

Because the cooling water pipe is connected to the automobile engine, the material of product must meet the requirements of high temperature, shock, and fatigue resistance. Through the contrast of engineering plastic properties, the material is selected as PA66 + 30% GF. It is a rare material that can meet the stringent requirements of automotive engine parts.

Considering the simplification of the model and calculation efficiency, the two brackets of product are removed. At first, Gambit is used to divide the tetrahedral mesh unit,

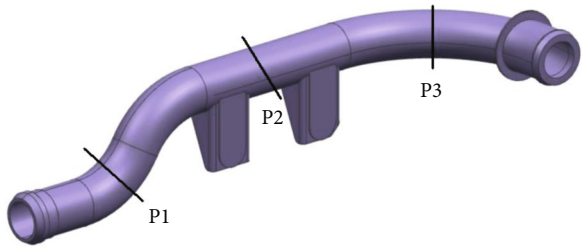

Figure 3: Model of cooling water pipe.

and then, the 3D mesh model is imported into Fluent for simulation calculation. For CAE simulation, the multifluid volume of fluid is adopted. Boundary conditions are specified as follows: the pressure and temperature of the inlet derive from the values of water injection; the pressure of the outlet is atmospheric pressure; no-slip boundary condition is used at the wall, and fixed temperature boundary condition is employed for the method of heat exchange; no-slip condition is applied at the solid-melt interface; Dirichlet boundary condition is specified at the water-melt interface. In addition, the numerical calculation of the flow field is the PISO algorithm, the underrelaxation factors are set to 0.2, and the time step of the iterative calculation is set to 10^{-5} s.

The molding method is short shot, and the main process parameters are short shot size A_s, melt temperature T_{me}, water pressure P_w, delay time t_d, and mold temperature T_{mo}, the value ranges of which are as follows: A_s [60, 68] (%); T_{me} [543, 593] (K); P_w [6, 10] (MPa); t_d [0, 4] (s); T_{mo} [313, 353] (K). Using the above process parameters for simulation calculations, hollowed core ratio H and wall thickness difference D at three different locations of the product are first obtained, and then, the average value is taken.

In this paper, DOE of Opt LHS is applied to get the training samples, the process of which is as follows. First, the numbers of design varies n are determined, and the sample numbers m are defined, respectively. Then, every coordinate space is divided into m intervals in n dimensions equally, of which every interval is named $[x_k^{i-1}, x_k^i]$. Finally, DOE of Opt LHS with varies n and sample numbers m are constituted by choosing m points randomly in interval according to the principle of every level studied only one [25]. For DOE of Opt LHS, the grade of horizontal value is loose, and the experimental numbers can be controlled artificially. Considering the time cost of calculation and accuracy of modeling comprehensively, the training samples of DOE of Opt LHS for cooling water pipe are 22, as shown in Table 1.

2.4.2. Build a Surrogate Model. Training samples were used to construct RSM, RBF, and Kriging surrogate models, so as to establish the nonlinear relationship between the process parameters and hollowed core ratio and wall thickness difference. For the RSM model, the order of the polynomial depends mainly on the number of design variables and sample points. In this study, there are five design variables and twenty-two sample points. Therefore, second-order polynomial functions are selected. In order to improve the precision and quality of the model, the term selection method is an exhaustive search. Although it requires the highest computational amount, the quality is the best. For the RBF model, the nonlinear radial basis function is selected as the Gauss function, of which the prediction curve is smooth. The smoothing filter is 0, and the maximum iterations to fit is 50. Furthermore, for the Kriging model, the fit type is anisotropic, the correlation function is Gaussian, and the maximum iterations to fit is 1000. Cross-validation is used to test the accuracy of the three models to determine whether the fitted surrogate model meets the accuracy requirements (see Section 3.2).

Table 1: DOE of Opt LHS.

Sample	A_s (%)	T_{me} (K)	P_w (MPa)	t_d (s)	T_{mo} (K)	H (%)	D (%)
1	61.9	593.0	8.5	2.3	318.7	55.9	27.9
2	66.1	578.7	10.0	2.9	332.1	55.3	23.3
3	67.6	574.0	7.9	2.5	351.1	52.4	26.1
4	61.1	576.3	7.5	0.0	330.1	55.8	26.6
5	65.7	552.5	6.4	3.2	334.0	49.2	26.5
6	60.8	571.6	6.2	2.7	322.5	52.0	26.7
7	63.1	590.6	9.1	1.3	349.2	56.9	32.3
8	63.8	569.2	9.8	0.8	314.9	56.1	28.7
9	65.3	564.4	6.8	1.0	313.0	50.0	27.6
10	64.2	547.8	9.2	3.1	347.3	54.7	22.6
11	66.5	554.9	6.6	0.4	341.6	48.6	33.0
12	67.2	585.9	8.3	0.6	328.2	54.7	25.8
13	62.3	543.0	8.1	1.1	326.3	53.3	25.8
14	65.0	559.7	9.4	0.2	345.4	54.9	20.8
15	61.5	562.1	7.0	1.7	353.0	52.8	24.5
16	60.0	566.8	9.6	2.1	335.9	58.3	23.0
17	64.6	588.2	6.0	1.5	339.7	57.9	21.2
18	66.9	583.5	7.1	3.4	320.6	50.7	20.5
19	60.4	545.4	7.3	3.8	337.8	55.9	26.3
20	68.0	550.1	8.9	1.9	324.4	52.8	21.7
21	63.4	557.3	8.7	3.6	316.8	55.8	18.8
22	62.7	581.1	7.7	4.0	343.5	51.7	18.7

2.4.3. Optimize by the PSO Algorithm. In order to ensure that the flow rate of water is sufficiently large, the hollowed core ratio should be as large as possible. In addition, the residual wall thickness distribution is also needed to be uniform, and the wall thickness difference should be controlled as small as possible. Therefore, the essence of this optimization problem is to find the process parameter combination with the largest hollowed core ratio and the smallest wall thickness difference in the feasible process space. This is a multiobjective optimization problem, and the mathematical model is as follows:

Find:

$$X = [A_s, T_{me}, P_w, t_d, T_{mo}]^T,$$

$$\text{Maximize} : \text{hollowed core ratio} H,$$

$$\text{Minimize} : \text{wall thickness difference} D,$$

$$\text{Subjected to constraint} : \text{waterpenetrationlength} \geq 409.3\text{mm}. \quad (17)$$

Within ranges:

$$\begin{aligned} 52.4 &\leq H, \\ 60 \leq A_s &\leq 68, \\ 543\text{K} \leq T_{me} &\leq 593\text{K}, \\ 6\text{MPa} \leq P_w &\leq 10\text{MPa}, \\ 0\text{s} \leq t_d &\leq 4\text{s}, \\ 313\text{K} \leq T_{mo} &\leq 353\text{K}. \end{aligned} \quad (18)$$

The PSO algorithm flow is shown in Figure 4. Furthermore, the optimization parameters are set as follows: the maximum iterations, 50; the number of particles, 50; the inertia, 0.9; the global increment, 0.9; the particle increment, 0.9; and the maximum velocity, 0.1.

2.4.4. Result Verification. The optimization process is a combination strategy including the DOE, surrogate model, and optimization algorithm, and errors are inevitable in the calculation process. Therefore, it is necessary to verify the final optimization results and analyze the accuracy of the optimization method.

3. Results and Discussion

3.1. Effects of Process Parameters on Hollowed Core Ratio. In WAIM, high-pressure water is injected into the mold cavity after the melt filling stage. As the rapid cooling effect of water on melt, a highly viscous membrane will be formed at the leading edge of the water. As shown in Figure 5, it demonstrates that the water penetrates into the core of the melt along the path of the least resistance, for which the hollow part is formed.

As shown in Figure 6, the hollowed core ratio decreases significantly with short shot size rising. This can be explained that rising short shot size will leave less space of water penetration, which increases residual wall thickness, or rather, hollowed core ratio decreases.

It can be seen from Figure 7 that the hollowed core ratio increases slightly as delay time increases. This is because increasing delay time will make melt's solidified layer thicker; on the other hand, the longer cooling time makes water penetration difficult.

As shown in Figure 8, the hollowed core ratio increases with melt temperature rising. This is caused by that rising melt temperature leads to reduce the viscosity of melt, which makes water penetration easier and more water penetrates to mold wall direction.

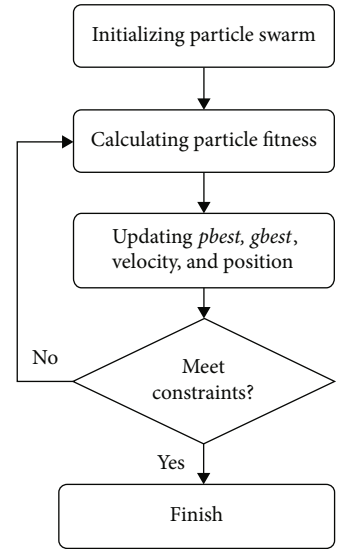

Figure 4: PSO algorithm flow.

Figure 9 shows that the hollowed core ratio increases with water pressure rising, which is very obvious. This is due to the fact that rising water pressure will lead water to squeeze the mold wall stronger, which makes residual wall thickness tend to decrease. Accordingly, the hollowed core ratio will increase.

As shown in Figure 10, the hollowed core ratio increases very little with mold temperature rising. This may be due to the fact that two contradictory phenomena occur when rising mold temperature: one is that the solidified layer of melt becomes thicker, which is likely to make residual wall thickness decrease; the other is that higher mold temperature makes water penetration easily, which increases residual wall thickness.

3.2. Cross-Validation of Surrogate Models. In this paper, cross-validation is adopted, which is an effective test method widely used in metamodeling techniques in support of engineering design optimization [8, 26]. The testing samples consist of 10 groups, and the accuracy of the three surrogate models is tested using two evaluation indicators: relative error (RE) and relative precision (RP). The smaller RE is, the littler the deviation degree between the predicted and actual values is. Meanwhile, the larger RP is, the higher the fitting degree is. RE and RP are calculated as follows:

$$\begin{aligned} \text{RE} &= \left| \frac{\widehat{y}_i - y_i}{y_i} \right| \times 100\%, \\ \text{RP} &= 1 - \left| \frac{\widehat{y}_i - y_i}{y_i} \right| \times 100\%. \end{aligned} \quad (19)$$

RE and RP of hollowed core ratio for the three models are shown in Table 2. The results indicate that for 10 testing samples, the RP of the RSM model for predicting hollowed core

Figure 5: Simulation result of water filling.

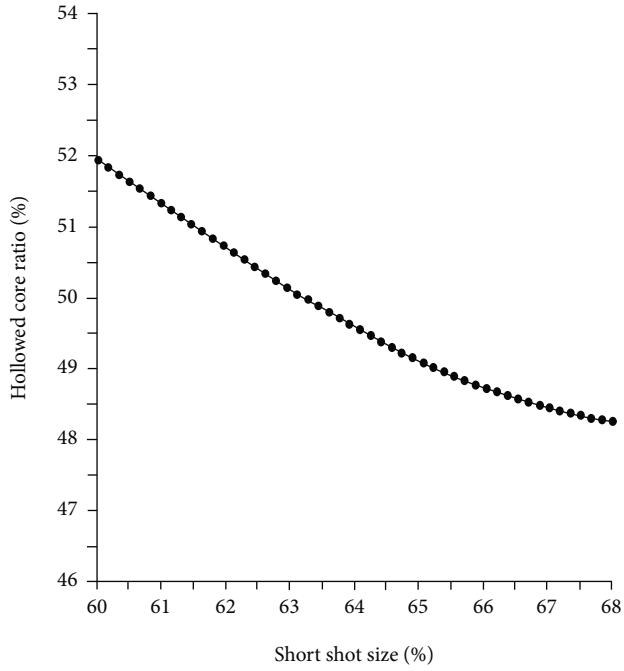

Figure 6: Effect of short shot size on hollowed core ratio.

ratio are all above 96%, with the maximum value of 99.6%, the minimum value of 96.8%, and the mean value of 98.5%. The RP of the RBF model are all above 97%, with the maximum value being 99.6%, the minimum value being 97.0%, and the mean value being 98.8%. Furthermore, the RP of the Kriging model are all above 95%, of which the maximum value is 98.7%, the minimum value is 95.3%, and the mean value is 97.2%. Overall, the prediction accuracy of the three models for hollowed core ratio is high, among which the RBF model has the strongest prediction ability, the RSM model is the second, and the Kriging model is the worst.

Table 3 is the RE and RP of wall thickness difference for the three models. It shows that the maximum RP of RSM, RBF, and Kriging models for wall thickness difference is 98.0%, 98.4%, and 98.5%, respectively; the minimum RP is 87.8%, 83.6%, and 81.0%; and the mean RP is 92.9%, 92.4%, and 90.5%. The predictive ability of RSM and RBF models is similar, while the Kriging model is the worst. Obviously, the prediction ability of the three models for wall thickness difference is weaker than that for the hollowed core ratio.

The comprehensive RP of RSM, RBF, and Kriging models for hollowed core ratio and wall thickness difference are 95.7%, 95.6%, and 93.9%, respectively, among which the prediction capabilities of RSM and RBF models are high and very close. Nevertheless, the Kriging model is significantly worse. The main reason is that the correlation function used in the Kriging model is a Gaussian, which is characterized by local interpolation. Compared with wall thickness difference, the hollowed core ratio of the cooling water pipe is a more important optimization object. Therefore, the RBF neural network with a stronger prediction ability of hollowed core ratio is used to couple the PSO algorithm for the multiobjective optimization problem.

3.3. Multiobjective Optimization. For this problem, the optimal design requires the hollowed core ratio as large as possible, and wall thickness difference as small as possible. However, in actual WAIM optimization, the two objects are difficult to meet at the same time. Namely, as the hollowed core ratio increases, wall thickness difference also increases. Considering that the improvement of any one object is at the expense of other objects, the optimal design of this problem is actually a Pareto solution that compromises hollowed core ratio and wall thickness difference. With the above combined optimization strategy of DOE of Opt LHS, RBF model, and PSO algorithm, multiobjective optimization on hollowed core ratio and wall thickness difference is performed. For the problems of traditional multiobjective optimization, multiobjective is usually transformed into a single objective. Nevertheless, there is no need to set the weights and proportionality coefficients of each target artificially with multiobjective PSO, which will automatically calculate Pareto optimal solutions. The number of simulations is confined in a predetermined value of 511 runs for this case study due to the computing cost of each simulation and the budget of time. Based on the results of 511 runs, the Pareto frontier for hollowed core ratio and wall thickness difference is shown in Figure 11.

After determining the Pareto frontier, the next step is to select the appropriate trade-off solution according to the actual engineering problem. In this problem, the hollowed core ratio of engine cooling water pipe needs to be large enough to provide more flow rate for cooling, and wall thickness difference should not be too large. According to the Pareto frontier, the hollowed core ratio of 58.4% at point P

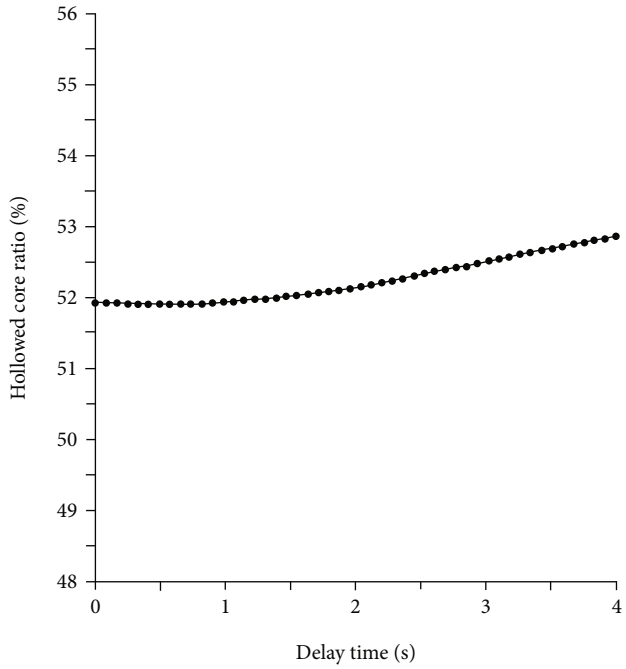

Figure 7: Effect of delay time on hollowed core ratio.

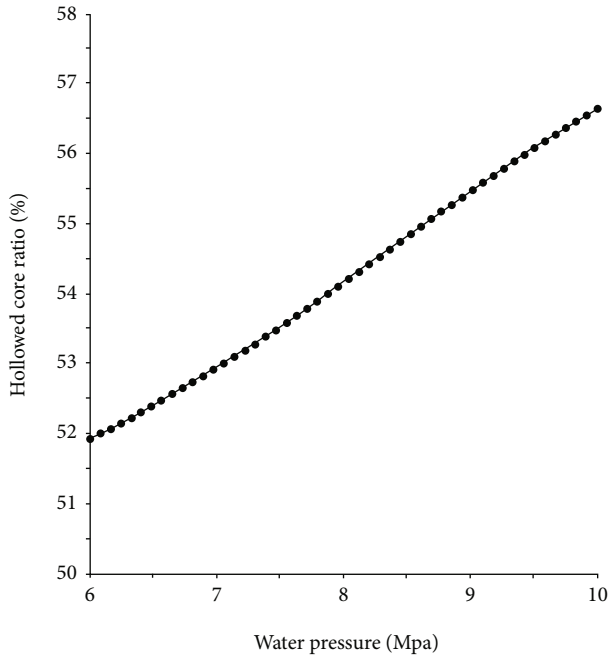

Figure 9: Effect of water pressure on hollowed core ratio.

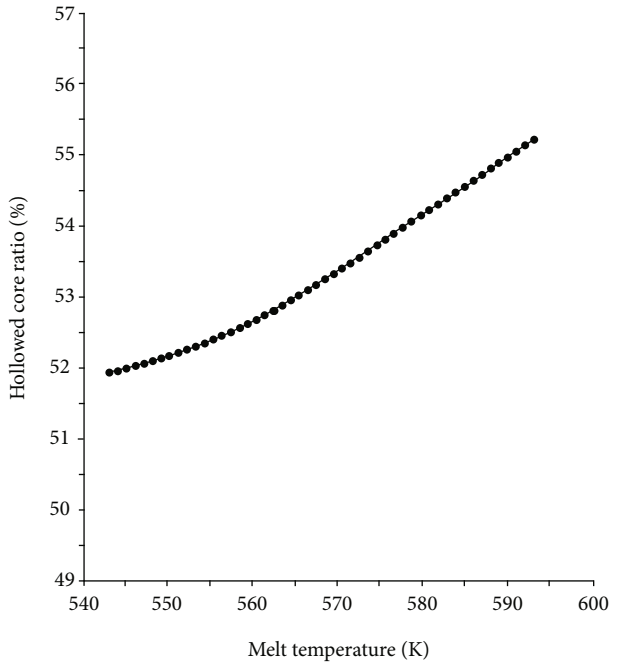

Figure 8: Effect of melt temperature on hollowed core ratio.

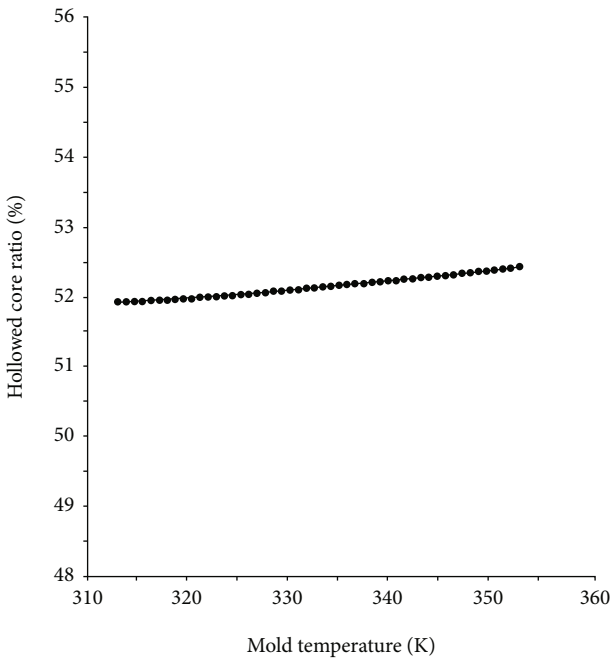

Figure 10: Effect of mold temperature on hollowed core ratio.

is very large in the whole Pareto solution set, and the wall thickness difference of 22.9% is also suitable. Therefore, point P is selected as the best solution, of which the corresponding process parameters are as follows: delay time, 2.4 s; melt temperature, 563 K; mold temperature, 330 K; short shot size, 60%; and water pressure, 10 MPa.

To verify the best solution of the hollowed core ratio and wall thickness difference obtained by hybrid optimization strategy, a confirmation experiment is absolutely necessary. As shown in Table 4, the comparison between the best solution and verification value demonstrates that the RE for the hollowed core ratio is 2.2%. In addition, the RE for wall thickness difference is slightly larger, 3%. The REs of hollowed core ratio and wall thickness difference are both small, which fully meet the accuracy requirements. As a result, it is easy to conclude that the hybrid optimization strategy has good

Table 2: The actual value, predicted value, RE, and RP of hollowed core ratio of the three models.

Sample	1	2	3	4	5	6	7	8	9	10	Mean
Actual value (%)	53.8	54.0	54.6	54.3	55.7	54.0	51.9	54.6	53.1	54.0	54.0
RSM predicted value (%)	54.2	54.7	55.3	55.1	56.7	54.2	52.8	55.1	54.8	54.9	54.9
RBF predicted value (%)	54.5	54.6	54.7	53.9	56.5	53.8	52.9	53.9	54.7	54.4	54.4
Kriging predicted value (%)	55.1	56.0	56.1	55.6	57.7	55.2	51.2	55.6	55.6	55.6	55.4
RSM											
RE (%)	0.7	1.3	1.3	1.5	1.8	0.4	1.7	0.9	3.2	1.7	1.5
RP (%)	99.3	98.7	98.7	98.5	98.2	99.6	98.3	99.1	96.8	98.3	98.5
RBF											
RE (%)	1.3	1.1	0.2	0.7	1.4	0.4	1.9	1.3	3.0	0.7	1.2
RP (%)	98.7	98.9	99.8	99.3	98.6	99.6	98.1	98.7	97.0	99.3	98.8
Kriging											
RE (%)	2.4	3.7	2.7	2.4	3.6	2.2	1.3	1.8	4.7	3.0	2.8
RP (%)	97.6	96.3	97.3	97.6	96.4	97.8	98.7	98.2	95.3	97.0	97.2

Table 3: The actual value, predicted value, RE, and RP of wall thickness difference of the three models.

Sample	1	2	3	4	5	6	7	8	9	10	Mean
Actual value (%)	25.7	23.4	24.6	25.0	25.8	27.1	26.7	20.3	23.1	20.3	24.2
RSM predicted value (%)	24.0	24.1	24.1	22.6	27.5	23.8	25.2	22.6	22.5	22.6	24.1
RBF predicted value (%)	23.0	22.8	23.3	20.9	26.2	23.4	23.4	20.9	21.3	20.9	22.6
Kriging predicted value (%)	20.8	20.5	25.5	23.8	28.5	25.5	26.3	23.8	23.8	23.8	24.2
RSM											
RE (%)	6.6	3.0	2.0	9.6	6.9	12.2	5.6	11.3	2.6	11.3	7.1
RP (%)	93.4	97.0	98.0	90.4	93.1	87.8	94.4	88.7	97.4	88.7	92.9
RBF											
RE (%)	10.5	2.6	5.3	16.4	1.6	13.7	12.4	3.0	7.8	3.0	7.6
RP (%)	89.5	97.4	94.7	83.6	98.4	86.3	87.6	97.0	92.2	97.0	92.4
Kriging											
RE (%)	19.0	12.4	3.6	4.8	10.5	5.9	1.5	17.2	3.0	17.2	9.5
RP (%)	81.0	87.6	96.4	95.2	89.5	94.1	98.5	82.8	97.0	82.8	90.5

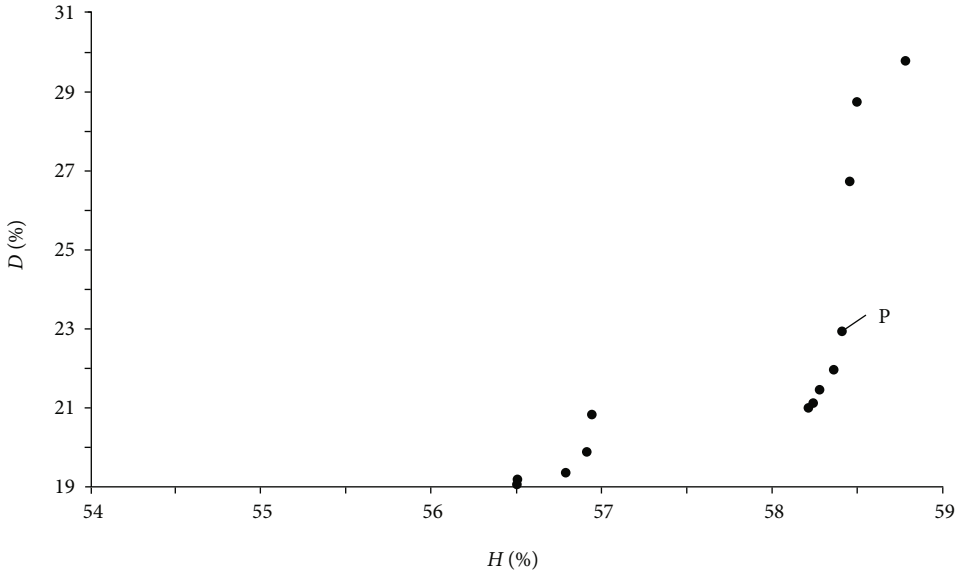

Figure 11: Pareto frontier.

Table 4: Comparison between the best solution and the verification value.

	A_s	T_{me}	P_w	t_d	T_{mo}	H (%)		RE	D (%)		RE
	%	K	MPa	s	K	Optimal	Verification	%	Optimal	Verification	%
Point P	60	563	10	2.4	330	58.4	59.7	2.2	22.9	23.6	3.0

adaptability to multiobjective optimization on hollowed core ratio and wall thickness difference.

4. Conclusions

In this paper, the residual wall thickness of the cooling water pipe was simulated by the CFD method. It was concluded that water pressure, short shot, and melt temperature were the most critical process parameters influencing residual wall thickness. Rising water pressure and short shot both would obviously decrease residual wall thickness, or rather, hollowed core ratio increased. On the contrary, the hollowed core ratio increased with melt temperature rising. Furthermore, delay time and mold temperature had little influence on the hollowed core ratio.

DOE of Opt LHS improved balance and spatial filling of sample points, and it was suitable for sample acquisition in plastic injection molding. As for the RP comparison of RSM, RBF, and Kriging models, the RBF model has the highest RP for hollowed core ratio. The comprehensive RP for hollowed core ratio and wall thickness difference of RSM and RBF models is very close and very high, while the RP of the Kriging model is relatively low. As a result, RBF was an effective model to fit the relationship between process parameters and residual wall thickness.

An efficient optimization methodology coupled with DOE of Opt LHS, RBF neural networks, and multiobjective PSO algorithm was adopted in maximizing hollowed core ratio and minimizing wall thickness difference. The optimization design requires that the hollowed core ratio is as large as possible, and the wall thickness difference is as small as possible. Through the confirmation experiment for the best solution, it shows that the RE for hollowed core ratio is 2.2%, and the RE for wall thickness difference is 3%. In conclusion, the combined optimization strategy can find the optimal solution of hollowed core ratio and wall thickness difference in the entire design space, and the accuracy also meets the requirements for WAIM.

Data Availability

All data used during the study appear in the submitted article, and no additional data are available.

Conflicts of Interest

The authors declare that they have no conflict of interest.

Acknowledgments

This work was supported by the National Natural Science Foundation of China (Grant No. 51741505) and Dr. Start-up Project of Shanghai Ocean University (Grant No. A2-2006-00-200370), for which the authors are very grateful.

References

[1] H. P. Park, B. S. Cha, and B. Rhee, "Experimental and Numerical Investigation of the Effect of Process Conditions on Residual Wall Thickness and Cooling and Surface Characteristics of Water- Assisted Injection Molded Hollow Products," *Advances in Materials Science and Engineering*, vol. 2015, Article ID 161938, 11 pages, 2015.

[2] T. Q. Kuang, K. Zhou, L. X. Wu, G.-F. Zhou, and L.-S. Turng, "Experimental study on the penetration interfaces of pipes with different cross-sections in overflow water-assisted coinjection molding," *Journal of Applied Polymer Science*, vol. 133, no. 1, p. 42866, 2016.

[3] H.-P. Park, B.-S. Cha, S.-B. Park et al., "A study on the void formation in residual wall thickness of fluid-assisted injection molding parts," *Advances in Materials Science and Engineering*, vol. 2014, Article ID 238251, 6 pages, 2014.

[4] H. P. Park and B. Rhee, "Effects of the viscosity and thermal property of fluids on the residual wall thickness and concentricity of the hollow products in fluid-assisted injection molding," *International Journal of Advanced Manufacturing Technology*, vol. 86, no. 9-12, pp. 3255–3265, 2016.

[5] S. SANNEN, P. van PUYVELDE, and J. O. Z. E. F. I. E. N. de KEYZER, "Defect occurrence in water-assisted injection-molded products: definition and responsible formation mechanisms," *Advances in Polymer Technology*, vol. 34, no. 1, 2015.

[6] T.-. Q. Kuang, J.-. Y. Pan, Q. Feng et al., "Residual wall thickness of water-powered projectile-assisted injection molding pipes," *Polymer Engineering and Science*, vol. 59, no. 2, pp. 295–303, 2018.

[7] Y. Yang, B. Yang, S. Zhu, and X. Chen, "Online quality optimization of the injection molding process via digital image processing and model-free optimization," *Journal of Materials Processing Technology*, vol. 226, pp. 85–98, 2015.

[8] S. A. Elsheikhi and K. Y. Benyounis, "Mathematical modeling and optimization of injection molding of plastics," *Reference Module in Materials Science and Materials Engineering*, pp. 1–16, 2017.

[9] S. J. Liu and Y. S. Chen, "The manufacturing of thermoplastic composite parts by water-assisted injection-molding technology," *Composites Part A: Applied Science and Manufacturing*, vol. 35, no. 2, pp. 171–180, 2004.

[10] H. X. Huang and Z. W. Deng, "Effects and optimization of processing parameters in water-assisted injection molding,"

Journal of Applied Polymer Science, vol. 108, no. 1, pp. 228–235, 2008.

[11] J. G. Yang, X. H. Zhou, and G. P. Luo, "Study of water penetration length and processing parameters optimization in water-assisted injection molding," *International Journal of Advanced Manufacturing Technology*, vol. 69, no. 9-12, pp. 2605–2612, 2013.

[12] H. Zhou, H. Liu, T. Kuang, Q. Jiang, Z. Chen, and W. Li, "Optimization of Residual Wall Thickness Uniformity in Short-Fiber-Reinforced Composites Water-Assisted Injection Molding Using Response Surface Methodology and Artificial Neural Network-Genetic Algorithm," *Advances in Polymer Technology*, vol. 2020, Article ID 6154694, 10 pages, 2020.

[13] J. G. Yang, X. H. Zhou, and Q. Niu, "Model and simulation of water penetration in water-assisted injection molding," *International Journal of Advanced Manufacturing Technology*, vol. 67, no. 1-4, pp. 367–375, 2013.

[14] F. Alkaabneh, M. Barghash, and Y. Abdullat, "A novel statistical analysis for residual stress in injection molding," *American Journal of Operations Reseatch*, vol. 6, no. 1, pp. 90–103, 2016.

[15] K. Li, S. L. Yan, Y. C. Zhong, W. Pan, and G. Zhao, "Multi-objective optimization of the fiber-reinforced composite injection molding process using Taguchi method, RSM, and NSGA-II," *Simulation Modelling Practice and Theory*, vol. 91, pp. 69–82, 2019.

[16] C. Li, F. L. Wang, Y. Q. Chang, and Y. Liu, "A modified global optimization method based on surrogate model and its application in packing profile optimization of injection molding process," *International Journal of Advanced Manufacturing Technology*, vol. 48, no. 5-8, pp. 505–511, 2010.

[17] S. Kitayama, K. Tamada, M. Takano, and S. Aiba, "Numerical optimization of process parameters in plastic injection molding for minimizing weldlines and clamping force using conformal cooling channel," *Journal of Manufacturing Processes*, vol. 32, pp. 782–790, 2018.

[18] B. Shiroud Heidari, A. Hedayati Moghaddam, S. M. Davachi, S. Khamani, and A. Alihosseini, "Optimization of process parameters in plastic injection molding for minimizing the volumetric shrinkage and warpage using radial basis function (RBF) coupled with the k-fold cross validation technique," *Journal of Polymer Engineering*, vol. 39, no. 5, pp. 481–492, 2019.

[19] T. W. Simpson, J. D. Poplinski, P. N. Koch, and J. K. Allen, "Metamodels for computer-based engineering design: survey and recommendations," *Engineering with Computers*, vol. 17, no. 2, pp. 129–150, 2001.

[20] H. X. Li, K. Liu, D. Y. Zhao, M. Wang, Q. Li, and J. Hou, "Multi-objective optimization for microinjection molding process parameters of biodegradable polymer stent," *Materials*, vol. 11, pp. 2321-2322, 2018.

[21] D. X. Su, J. Zhao, Y. Wang, and M. J. Qu, "Kriging-based orthotropic closure for flow-induced fiber orientation and the part stiffness predictions with experimental investigation," *Polymer Composites*, vol. 40, no. 10, pp. 3844–3856, 2019.

[22] R. J. Bensingh, R. Machavaram, S. R. Boopathy, and C. Jebaraj, "Injection molding process optimization of a bi-aspheric lens using hybrid artificial neural networks (ANNs) and particle swarm optimization (PSO)," *Measurement*, vol. 134, pp. 359–374, 2019.

[23] H. S. Yan and Z. G. Shang, "Product design time forecast using relative entropy kernel regression," *International Journal of Industrial Engineering-Theory Applications and Practice*, vol. 26, pp. 343–360, 2019.

[24] P. Zhao, Z. Y. Dong, J. F. Zhang et al., "Optimization of injection-molding process parameters for weight control: converting optimization problem to classification problem," *Advances in Polymer Technology*, vol. 2020, Article ID 7654249, 9 pages, 2020.

[25] J. G. Yang, S. R. Yu, and M. Yu, "Prediction of process parameters of water-assisted injection molding based on inverse radial basis function neural network," *Polymer Engineering and Science*, 2020.

[26] G. G. Wang and S. Shan, "Review of metamodeling techniques in support of engineering design optimization," *Journal of Mechanical Design*, vol. 129, no. 4, pp. 370–380, 2007.